Frequency Reprogrammable $Al_{0.7}Sc_{0.3}N$ Acoustic Delay Line with up to 13.5 % Bandwidth

Onurcan Kaya, Xuanyi Zhao, Cristian Cassella
Electrical and Computer Engineering
Northeastern University
Boston, USA

***Summary*—In this study, a 30% Scandium doped Aluminum Nitride ($Al_{0.7}Sc_{0.3}N$) Two-Dimensional-Resonant-Rods (2DRRs) based Acoustic Delay Line (ADL) is presented. The reported ADL has two distinctive features. Firstly, it shows a record-high bandwidth (BW) up to 13.5 %, which can hardly be achieved by any Lamb Wave or Surface Acoustic Wave counterparts. Secondly, when selecting proper electrical matching conditions and thanks to the unique dispersion features of its metamaterial structure, the reported ADL can be programmed to selectively operate with large BWs around 4 different frequencies (115 MHz, 150 MHz, 210 MHz, and 300 MHz), demonstrating an extraordinary frequency re-programmability that has never been allowed by any prior ADL counterparts.**

Keywords—Acoustic Delay Line, Acoustic Metamaterials, Aluminum Scandium Nitride, Two-Dimensional Resonant Rods

I. Introduction

The recent improvements in CMOS-compatible circulators [1] pave the wave towards mobile communication systems that rely on full-duplex radios (FDRs) to achieve the highest possible spectral efficiency. In such radios, self-interference (SI) cancellation networks, including a set of delay lines, are required to overcome the FDRs' performance degradations caused by portions of the high power transmitted signals reaching and saturating the FDRs' receiving module. In the last decades, several Surface Acoustic Wave (SAW) [2] and Lamb Wave (LW) [3] delay lines have been demonstrated. However, none of them has shown a wide enough fractional bandwidth and low enough insertion loss to be used in SI cancellation networks of wideband FDRs, while ensuring CMOS compatibility.

Conventional delay lines consist of frequency selective input/output transducers and a wideband delay element between them [3-6]. This structure prevents from relying on the inherently wideband frequency response of the delay element, even generating significant challenges whenever electrical components must be used to electrically match the resonant and narrowband input and output transducers to 50 Ω. In our earlier studies [7], we showed that a delay line consisting of wide-band input/output transducers and a frequency selective element between them based on a Two-Dimensional Resonant Rod (2DRR) acoustic metamaterial structure can exhibit low-loss and large fractional bandwidths, which is hardly achievable by the existing SAW and LW counterparts.

In this work, we report the first frequency reprogrammable Aluminum Scandium Nitride (AlScN) acoustic delay line (ADL) with up to 13.5% 3-dB fractional bandwidth (BW). Thanks to its acoustic metamaterial structure, formed by a forest of locally resonant rods, the reported ADL can operate at four different frequencies (115 MHz, 150 MHz, 210 MHz, and 300 MHz), each one corresponding to the center frequency of an acoustic passband generated by the metamaterial structure. This unique feature enables an unprecedented frequency re-programmability never achieved by any LW or SAW counterparts. The performance of the reported ADL has been assessed through both Finite Element Methods (FEM) and measurements. In particular, the raw performance of the reported ADL has been evaluated when considering optimal frequency-independent input and output terminal impedances. Yet, the ADL reported here can be matched to any desired input/output impedances. In this regard, the 50 Ω matched performance of the reported ADL is also evaluated by using pairs of realistic matching networks with inductors having quality factors (Qs) of 100. Despite a slight decrease in performance due to the matching networks, the 50-ohm matched ADL reported here shows a fractional bandwidth up 13.5 % and a minimum insertion loss of ~ 8 dB.

II. Methods/Results

The presented device has two wideband input/output terminals and a corrugated structure between them (Fig. 1-a).

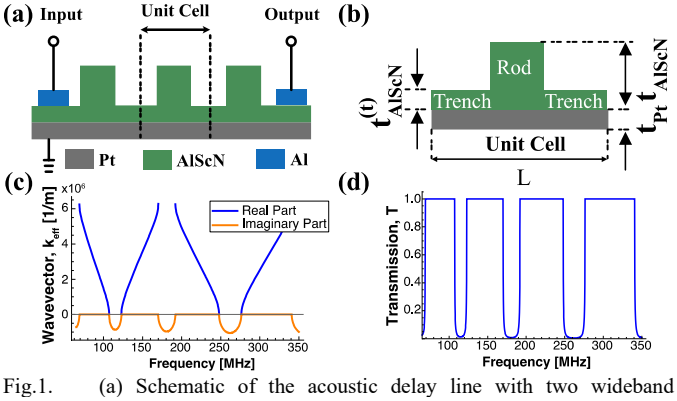

Fig.1. (a) Schematic of the acoustic delay line with two wideband input/output terminals and a corrugated structure in between them. (b) The unit cell of the corrugated structure. (c) Real and imaginary part of the analytically calculated k_{eff} for the reported ADL. d) Analytically calculated trend of T vs. frequency for the reported ADL.

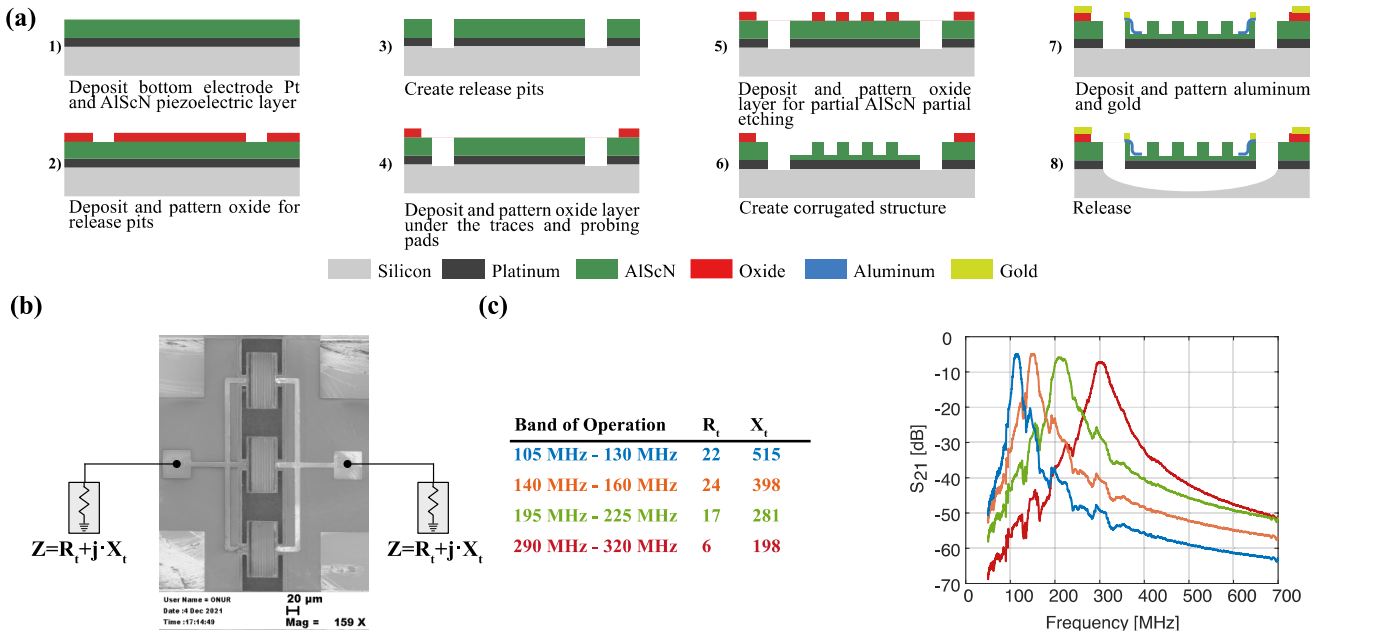

Fig.2. (a) Fabrication flow for the reported ADL. (b) SEM image of the fabricated ADL in between two terminals having optimal frequency-independent complex impedances. (c) Four different bands of operation along with the related resistance (R_t) and reactance (X_t) values and the resulting insertion loss. Depending on the complex impedance of terminals a single device can be re-programmed to operate within four different frequency bands.

The corrugated structure consists of 8 resonant rods connected by thin trenches. Depending on the dimensions and on the mechanical properties of its unit cell (Fig. 1-b), the propagation wavevectors of both longitudinal and shear modes (k_{eff}) become imaginary in certain frequency bands, creating regions where the propagation of real energy is no longer possible. This also allows manipulating the wave speed of both longitudinal and shear modes, providing the means to slow the acoustic propagation down when operating within any passbands. The analytically derived trends of the propagation vector (k_{eff}) and of the acoustic transmission coefficient (T) relative to the presented device have been estimated following the procedure discussed in [8] and are also shown here (Fig. 1-c and Fig. 1-d). As evident from Fig. 1-d, the presented device exhibits wide acoustic passbands centered around the four frequencies of interest in this work. It should be noted that the electrical bandwidth of the reported ADL is lower than the bandwidth of T, being ultimately set by the Bode-Fano limit relative to the ADL's electrical matching.

The reported ADL has been fabricated using a 500 nm thick (t_{AlScN}=500 nm) Aluminum Scandium Nitride ($Al_{0.7}Sc_{0.3}N$) film on top of a 100 nm thick (t_{Pt}=100 nm) Platinum layer. The corrugation is formed by partially etching 4/5 of the $Al_{0.7}Sc_{0.3}N$ film ($t^{(t)}_{AlScN}$= 100 nm). Then, the input/output electrodes were formed by patterning a 140 nm thick Aluminum layer. Finally, the electrical routing and probing pads were formed by patterning a 300 nm thick gold layer. The detailed fabrication flow is summarized in Fig. 2-a. The Scanning Electron Microscope (SEM) picture of the fabricated device is shown at the center of Fig. 2-b, between two terminals having optimal frequency-independent impedances. As evident, the reported ADL consists of an array of three identical electrically coupled devices to facilitate the electrical matching of its terminals to any desired impedances. Thanks to the multiple acoustic passbands generated by the acoustic metamaterial structure, the reported ADL can operate in 4 different frequency bands depending on the resistance (R_t) and reactance (X_t) values of its terminals. Related complex impedances along with the resulting insertion losses in each band of operation are given in Fig.2-c.

The performance of the reported ADL has been also analyzed by using realistic matching networks to match its optimum terminations to 50 Ω. In this regard, Fig.3-a shows the reported device between different pairs of matching networks, each one tailored to match the reported ADL for optimal operation within one of its acoustic passbands. Also, each matching network assumes three inductors with Qs of 100 and one capacitor. The closely matching FEM simulated and measured results of the presented ADL, after matching its terminals to 50 Ω, are given in Fig. 3-b,c. Fig.3-b shows the insertion loss relative to all four bands of operation in the same plot while Fig. 3-c focuses on each one of these bands, reporting the corresponding insertion loss (on the left axis) and group delay (on the right axis). Finally, the effect of the matching networks on the electrical performance of the reported ADL is analyzed in Fig. 3-d by comparing the responses of the 50 Ω-matched ADL with those shown in Fig. 2-c.

III. DISCUSSION/INTERPRETATION

The reported ADL can operate within four different passbands centered around 115 MHz, 150 MHz, 210 MHz, and 300 MHz, which are originated from the acoustic metamaterial structure (Fig.2-b). When the reported ADL is matched to 50 Ω, the 3 dB fractional bandwidth of each passband is 11.2 %, 11.3 %, 13.5%, and 8.7 % with a minimum recorded loss of ~8 dB. The measured group delay varies between ~70 ns and ~30 ns (Fig. 3-c). We speculate that such a large loss is due to

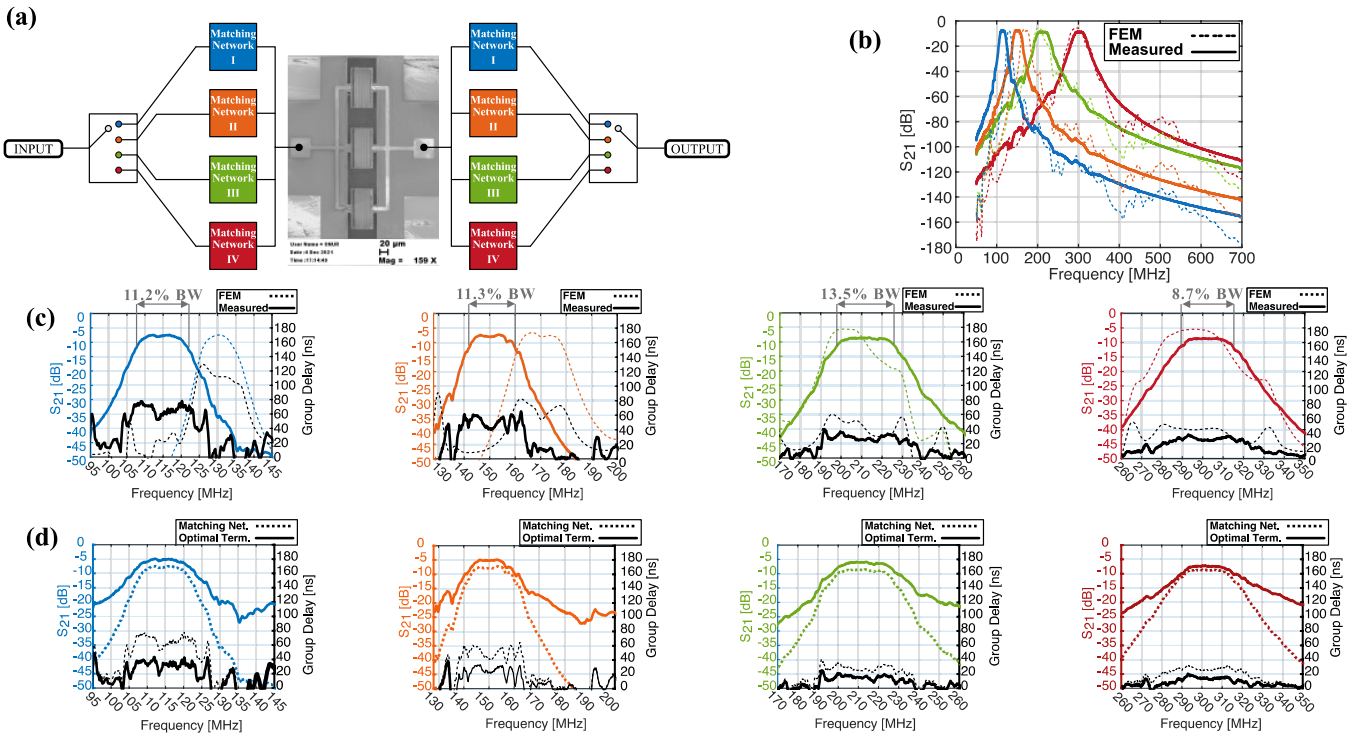

Fig.3. (a) SEM image of the fabricated ADL connected to the simulated matching networks we used for the different ADL's passbands. Depending on the employed matching networks, a single device can be re-programmed to operate within different frequency bands. (b) Insertion loss of the FEM-simulated (dashed line) and measured response (solid line) of the ADL, after matching to 50 Ω within different passbands. (c) Close-up view of each passband of the FEM-simulated (dashed line) and measured device (solid line), showing the corresponding insertion loss and group delay. (d) Comparison of the performance of the reported ADL with matching networks (dashed line) and with terminals having optimal frequency-independent complex impedances (solid line)

excessive amounts of electrical loading, thus being improvable by further engineering the ADL's metal routing.

As can be seen from Fig.3-d, by adding matching networks on both sides to match the optimal terminal impedances identified in Fig.2-b to 50 Ω, the response bandwidth slightly decreases (e.g. it is a chain of 3 lossy frequency selective components). In addition, adding matching networks increases the group delay by introducing electrostatic delay. Nevertheless, the net group delay contributed by the reported ADL is ~38 ns, ~30 ns, ~20 ns, and ~20 ns at the center of each passband, respectively. It should be noted that using matching networks allows for achieving higher out-of-band rejection since three frequency selective components (i.e., the reported ADL and two matching networks) are cascaded. However, this enhancement does not alter the validity of any claims made in this paper about BW and group delay.

Our measurements reveal two distinctive features of the presented ADL. Firstly, the high bandwidths achieved by our reported ADL would be hardly achievable by conventional LW or SAW counterparts. The bandwidth of the reported ADL is compared with the ones of recent LW or SAW-based counterparts [3-6] in Fig. 4. Secondly, since the reported ADL can obtain multiple acoustic passbands in a single microfabricated device thanks to the unique dispersion characteristics of its metamaterial structure, it can be programmed with proper electrical matching conditions to selectively operate around four different frequencies with large BWs that have never been allowed by any prior ADL counterparts.

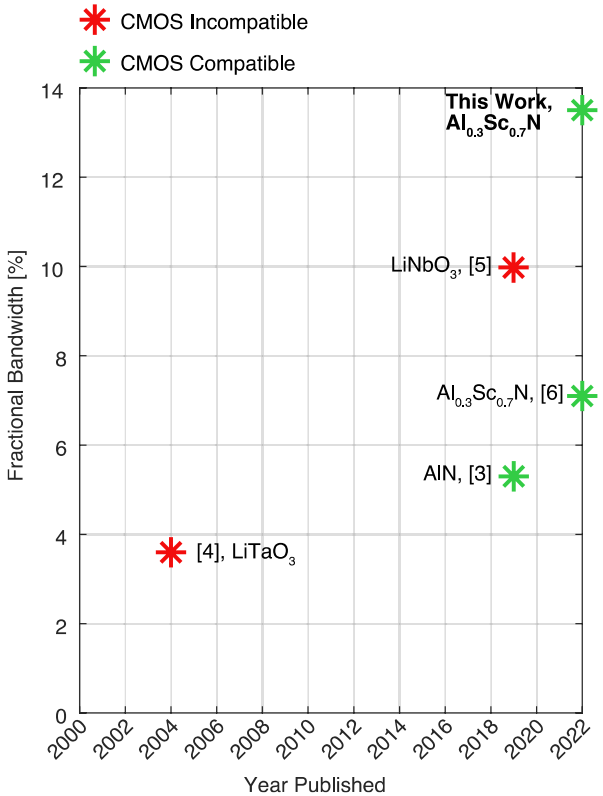

Fig.4. Comparison of the bandwidth of the reported delay line with several CMOS compatible and incompatible delay lines from the literature.

IV. Conclusions

This study presents the first frequency reprogrammable acoustic metamaterial-based AlScN ADL. The reported ADL can operate around four different frequencies within the Ultra-High-Frequency (UHF) range, exhibiting 3 dB fractional bandwidths up to 13.5%.

Acknowledgment

This work was supported by the DARPA WARP (HR0011-20-S-0027) program. The authors wish to thank the staff of the George J. Kostas Nanoscale Technology and Manufacturing Research Center at Northeastern University and the staff of the Center for Nanoscale Systems at Harvard University for assistance in the device fabrication.

References

[1] Y. Yu *et al.*, "Highly-Linear Magnet-Free Microelectromechanical Circulators," *Journal of Microelectromechanical Systems,* vol. 28, no. 6, pp. 933-940, 2019, doi: 10.1109/jmems.2019.2947903.

[2] R. Lu, Y. Yang, A. E. Hassanien, and S. Gong, "Gigahertz Low-Loss and High Power Handling Acoustic Delay Lines Using Thin-Film Lithium-Niobate-on-Sapphire," *IEEE Transactions on Microwave Theory and Techniques,* vol. 69, no. 7, pp. 3246-3254, 2021, doi: 10.1109/TMTT.2021.3074918.

[3] R. Lu, S. Link, S. Zhang, M. Breen, and S. Gong, "Aluminum Nitride Lamb Wave Delay Lines With Sub-6 dB Insertion Loss," *Journal of Microelectromechanical Systems,* vol. 28, no. 4, pp. 569-571, 2019, doi: 10.1109/JMEMS.2019.2919031.

[4] S. Lehtonen, V. P. Plessky, C. S. Hartmann, and M. M. Salomaa, "SPUDT filters for the 2.45 GHz ISM band," *IEEE Transactions on Ultrasonics, Ferroelectrics, and Frequency Control,* vol. 51, no. 12, pp. 1697-1703, 2004, doi: 10.1109/TUFFC.2004.1386687.

[5] T. Manzaneque, R. Lu, Y. Yang, and S. Gong, "Low-Loss and Wideband Acoustic Delay Lines," *IEEE Transactions on Microwave Theory and Techniques,* vol. 67, no. 4, pp. 1379-1391, 2019, doi: 10.1109/tmtt.2019.2900246.

[6] S. Shao, Z. Luo, Y. Lu, A. Mazzalai, C. Tosi, and T. Wu, "Low Loss $Al_{0.7}Sc_{0.3}N$ Thin Film Acoustic Delay Lines," *IEEE Electron Device Letters,* vol. 43, no. 4, pp. 647-650, 2022, doi: 10.1109/LED.2022.3152908.

[7] O. Kaya, X. Zhao, and C. Cassella, "An Aluminum Scandium Nitride ($Al_{0.64}Sc_{0.36}N$) Two-Dimensional-Resonant-Rods Delay Line with 7.5% Bandwidth and 1.8 dB Loss," in *2022 IEEE 35th International Conference on Micro Electro Mechanical Systems Conference (MEMS)*, 9-13 Jan. 2022 2022, pp. 1018-1021, doi: 10.1109/MEMS51670.2022.9699475.

[8] X. Zhao, L. Colombo, and C. Cassella, "Aluminum nitride two-dimensional-resonant-rods," *Applied Physics Letters,* vol. 116, no. 14, 2020, doi: 10.1063/5.0005203.